

Tuning optical band gap of vertically aligned ZnO nanowire arrays grown by homoepitaxial electrodeposition

Savarimuthu Philip Anthony, Jeong In Lee, and Jin Kon Kim^{a)}

National Creative Research Center for Block Copolymer Self-Assembly and Department of Chemical Engineering, Pohang University of Science and Technology, Kyungbuk 790-784, Korea

(Received 20 December 2006; accepted 31 January 2007; published online 7 March 2007)

Vertically aligned ZnO nanowire arrays are grown homoepitaxially on the ZnO seeded indium tin oxide substrate by electrochemical deposition from aqueous solution at low temperature (70 °C) without using any template. ZnO nanowires exhibit single crystalline, wurtzite crystal structure determined by transmission electron microscopy and powder x-ray diffraction. The ZnO nanowire arrays show high transmittance in the visible wavelengths. Interestingly, the optical band gap of the ZnO nanowire arrays has been tuned by simply changing zinc salts in the electrodeposition from aqueous solution. © 2007 American Institute of Physics. [DOI: 10.1063/1.2711419]

One-dimensional semiconductor nanostructures such as rods, wires, belts, and tubes have attracted much attention due to their unique optical and electronic properties useful in future electronics and photonics.¹⁻³ Among many oxide semiconductors, ZnO, a wide direct band gap ($E_g = 3.37$ eV) semiconductor with large exciton binding energy (60 meV), has been extensively investigated because of its great potential for piezoelectric transducers, optical waveguides, surface acoustic wave devices, phosphors, transparent conducting oxides, chemical and gas sensors, spin functional devices,⁴ blue light-emitting diodes,⁵ and dye-sensitized oxide semiconductor solar cell.⁶ ZnO nanowires have been prepared by various methods: chemical vapor deposition,⁷ metal-organic chemical vapor deposition,⁸ metal-organic vapor-phase epitaxy,⁹ and hydrothermal deposition.^{10,11}

Solution methods such as hydrothermal and electrodeposition are of particular interest for the growth of vertically aligned ZnO nanowire arrays due to low cost, environmentally friendly, and low temperature growth. Moreover, the crystal morphology and the aspect ratio of wires can be easily tuned, without using template just by controlling the concentration of Zn^{2+} precursor. Electrochemically, ZnO nanopillars were grown by heteroepitaxial deposition on a single crystalline Au substrate¹² and on a (0001)-GaN-coated (0001) sapphire substrate;¹³ where phase matching is important for the growth of vertical orientation, and by depositing Zn in the pores of anodic alumina membrane followed by oxidization to ZnO.¹⁴ Electrodeposited ZnO films or nanostructures have shown variations in the optical band gap depending on the voltage applied, type and concentration of zinc salts used, and the structural morphology obtained.¹⁵⁻¹⁸ It is known that the use of ZnO seed layer has been shown to promote and improve the vertical alignment of ZnO nanowire growth by nucleation effect in hydrothermal method.¹¹ Hence, the ZnO seed layer approach could also be extended to electrochemical deposition method for the growth of vertically aligned ZnO nanowires. This method has some advantages over heteroepitaxial growth on Au and GaN, where single crystalline structures of Au and GaN substrates are

required. Since the optical band gap shift of ZnO would be interesting because of the tunability of optoelectronic properties, electrochemical method could be a simple approach to tune the optical band gap of ZnO nanowires.

In this letter, fabrication of vertically aligned ZnO nanowires homoepitaxially on the ZnO seeded indium tin oxide (ITO) substrates using electrochemical deposition from aqueous solution at low temperature (70 °C) has been presented. The grown nanowires show good optical transparency and preferential *c*-axis orientation. Furthermore, the optical band gap of the aligned ZnO nanowires was easily tuned by using different zinc salts. The ZnO nanowires show single crystalline structure investigated by high resolution transmission electron microscope (HRTEM) and x-ray diffraction. The possible reason for the optical band gap shift of nanowire arrays fabricated from different zinc salts is discussed.

ZnO seed layer was prepared by spin coating the saturated methanol solution of $Zn(CH_3COO)_2 \cdot 2H_2O$ on ITO and heated at 350 °C for 30 min. The electrochemical growth of vertically aligned ZnO nanowires onto ZnO seed layer was carried out at -0.9 V versus Ag/AgCl reference electrode by using 5 mM zinc perchlorate ($Zn(ClO_4)_2$) with lithium perchlorate as a supporting electrolyte or 5 mM zinc nitrate ($Zn(NO_3)_2$) solution with potassium chloride as a supporting electrolyte. The 5 mM concentration has been chosen to obtain adequate electrodeposition rate of the ZnO without affecting the nanowire morphology. In $Zn(ClO_4)_2$ solution, H_2O_2 was used as oxygen precursor and the concentration ratio between H_2O_2 and Zn^{2+} has been maintained to 0.5. The morphology and size of the ZnO nanowires were investigated by field emission scanning electron microscopy (FESEM) (Hitachi, S-4800, operated at 5 kV), and single crystallinity of ZnO nanowires was investigated by HRTEM (JEM 2100F, operated at 200 kV). The crystal structure of the prepared ZnO nanowire was observed using x-ray diffraction (XRD) (Mac Science, M18X^{CE}) with Cu $K\alpha$ radiation. Optical absorption properties for the nanowire arrays have been recorded by using Carry 5000 UV-vis-near-infrared double beam spectrophotometer.

Figure 1(a) shows SEM images of ZnO seeds prepared on the ITO substrate, which appears a number of nanoparticles of ZnO randomly distributed on the surface of the substrate. Figures 1(b) and 1(c) show the surface morphology

^{a)} Author to whom correspondence should be addressed; electronic mail: jkkim@postech.ac.kr

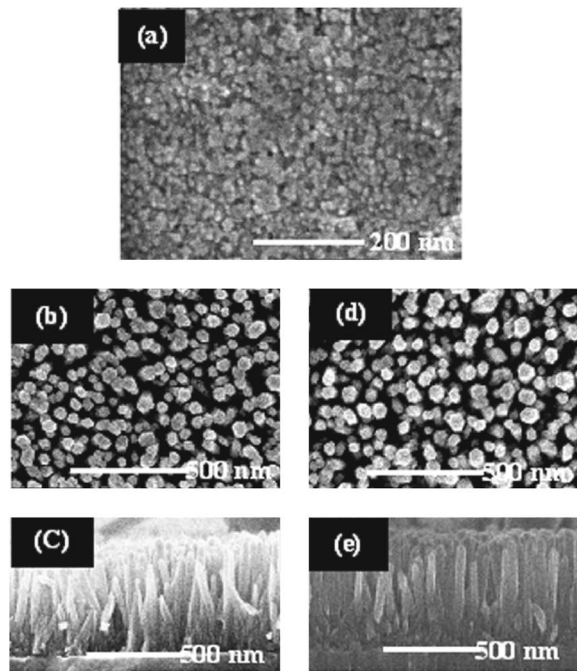


FIG. 1. FESEM images of (a) plan view of the ZnO seeds prepared on an ITO substrate, [(b) and (c)] plan view and cross-sectional images of ZnO nanowires fabricated from $\text{Zn}(\text{ClO}_4)_2$ solution (0.005M) and [(d) and (e)] plan view and cross-sectional images of ZnO nanowires fabricated from $\text{Zn}(\text{NO}_3)_2$ solution (0.005M).

and side view of ZnO nanowires grown onto ZnO seeds by electrodeposition from $\text{Zn}(\text{ClO}_4)_2$ solution, whereas Figs. 1(d) and 1(e) show the surface morphology and side view of ZnO nanowires grown from $\text{Zn}(\text{NO}_3)_2$ solution. Electrodeposition of ZnO on the bare ITO substrate (namely, without ZnO seeds) from $\text{Zn}(\text{ClO}_4)_2$ and $\text{Zn}(\text{NO}_3)_2$ solutions forms loosely packed and randomly aligned ZnO nanorods.¹⁸ It is seen from Figs. 1(b)–1(e) that electrodeposition of ZnO from $\text{Zn}(\text{ClO}_4)_2$ and $\text{Zn}(\text{NO}_3)_2$ solutions on the ZnO seeded ITO substrate leads to the vertically aligned nanowire arrays with hexagonal packing over the entire ITO substrate. This clearly demonstrates that the ZnO seeds improve the alignment as well as density of ZnO nanowires. The length of nanowires has been increased by increasing the electrodeposition time, whereas the diameter of the nanowire does not change with the electrodeposition time. Typically, nanowires grown for 40 min from 5 mM solution exhibit diameter and length of 40–70 and 500 nm, respectively. The diameter of ZnO nanowires can be varied by adjusting the solution concentrations. For instance, when 1 mM of zinc nitrate solution was used, nanowires with smaller diameter (25–50 nm) are obtained. But, when the concentration of the solution was increased (50, 100 mM), the diameter of the nanowires also increased. The nanowires were joined together to look like film morphology due to the faster rate of deposition. The crystal structure of the ZnO nanowires has been investigated by powder XRD. ZnO nanowire arrays fabricated from $\text{Zn}(\text{ClO}_4)_2$ and $\text{Zn}(\text{NO}_3)_2$ solutions on the ZnO seeded ITO substrate revealed only a peak at 34.38° corresponding to (0002) of the wurtzite structure of ZnO, indicating that the nanowires are preferentially oriented in *c*-axis direction.

Figures 2(a)–2(e) show the HRTEM image of nanowires fabricated from $\text{Zn}(\text{ClO}_4)_2$ and $\text{Zn}(\text{NO}_3)_2$ solutions, respectively. The lattice spacing of 0.26 nm corresponds to the *d* spacing of (0002) crystal planes, confirming the XRD analysis that ZnO nanowires are preferentially oriented in the *c*-axis direction. No dislocations or stacking faults are observed in all areas examined. However, it does not indicate that there are no other types of defects in the synthesized ZnO nanowire arrays, since defects such as vacancy or interstice may not be visible in the HRTEM observation. The sharp diffraction spots in the selected area electron diffraction pattern, as shown in Figs. 2(c) and 2(f), indicate the single crystal nature of the nanowires fabricated from $\text{Zn}(\text{ClO}_4)_2$ and $\text{Zn}(\text{NO}_3)_2$ solutions.

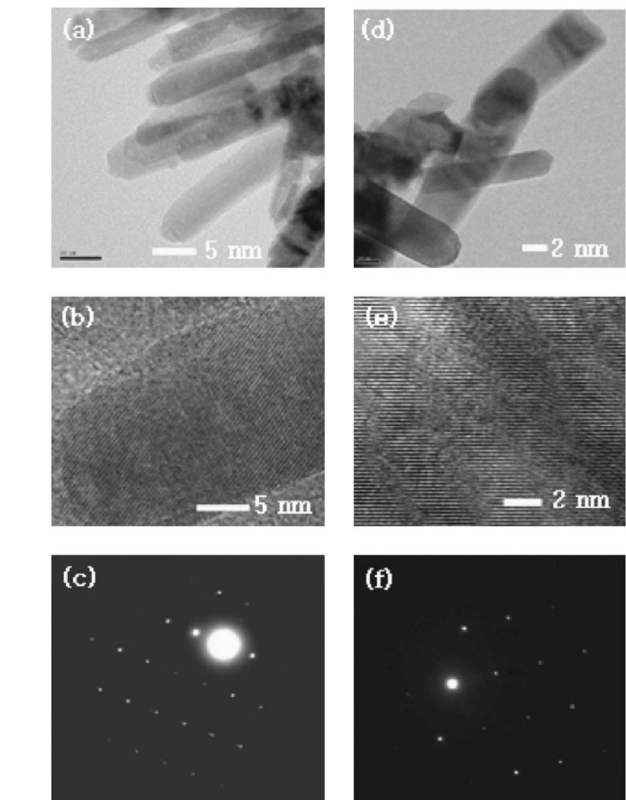


FIG. 2. [(a), (b), (d), and (e)] High-resolution TEM images and [(c) and (f)] selected area diffraction patterns of ZnO nanowire arrays grown from [(a), (b), (c)] $\text{Zn}(\text{ClO}_4)_2$ salt and [(d), (e), (f)] $\text{Zn}(\text{NO}_3)_2$ salt.

Figure 3(a) shows the optical transmission spectra of the nanowires fabricated from $\text{Zn}(\text{ClO}_4)_2$ and $\text{Zn}(\text{NO}_3)_2$ solutions and annealed samples at 400°C in air. Optical transparency of the ZnO is closely related to the roughness of the surface and the existence of defects such as pits and voids.¹⁹ Electrochemically deposited thick, compact films of ZnO with smooth surface show good optical transparency, while noncompact films having rough or porous surface show lesser transparency as the wavelength decreased.¹⁷ However, electrochemically fabricated nanowires from $\text{Zn}(\text{ClO}_4)_2$ and $\text{Zn}(\text{NO}_3)_2$ solution on the ZnO seeded ITO substrate, though having air gaps between the nanowires, exhibit good transparency in the visible range and a sharp absorption onset around 360–380 nm. This is attributed to the good crystalline characteristics of the nanowires.

Optical band gap of ZnO has been reported from 3.27 eV for the single crystal to 3.55 eV for the electrodeposited films.²⁰ The electrodeposited ZnO films or nanostructures exhibit band gap between 3.3 and 3.55 eV, depending on the structural morphologies and crystal defects. Assuming an absorption coefficient $\alpha \propto -\ln T$ (*T* is transmittance) corresponding to a direct band gap of ZnO,²¹ the band gap of

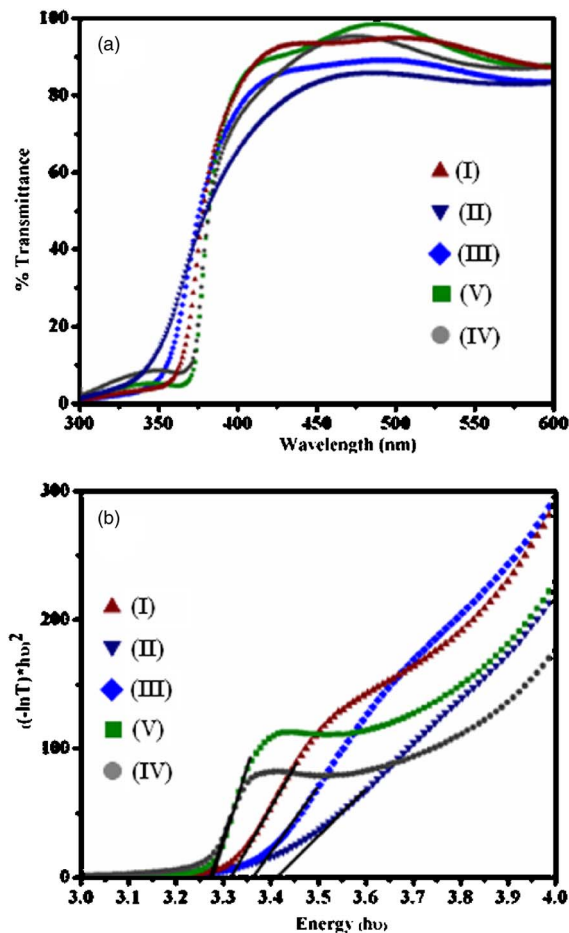


FIG. 3. (Color online) (a) Optical transmission spectra and (b) plot of $(\alpha hv)^2$ vs photon energy of ZnO nanowire arrays electrodeposited from (I) $Zn(ClO_4)_2$ solution, (II) $Zn(NO_3)_2$ solution, (III) $Zn(NO_3)_2$ solution in the presence of hydrogen peroxide, and [(IV) and (V)] annealing treatment under air at 400 °C for 1 h for (I) and (II), respectively.

the ZnO nanowires is estimated from the linear fit in plot of $(\alpha hv)^2$ against the energy $h\nu$, as shown in Fig. 3(b). The nanowires fabricated from $Zn(NO_3)_2$ solution exhibit optical band gap of 3.42 eV, whereas those from $Zn(ClO_4)_2$ solution show optical band gap of 3.32 eV. ZnO nanowire arrays fabricated from $Zn(NO_3)_2$ solution in the presence of hydrogen peroxide show optical band gap of 3.36 eV. On the other hand, when annealed at 400 °C under air, optical band gap of the nanowires redshift to 3.27 eV regardless of the anions.

Doping ZnO with transition or nontransition metal ions²² and size variation exhibit shift in the optical band gap.²³ The reason for the optical band gap variation of ZnO nanowire arrays grown by electrodeposition from different zinc salts is not yet clear. The influence of impurities such as oxychlorides and hydroxides, which could form during electrodeposition, on the optical band gap has been ruled out because the nanowires exhibit single crystalline characteristics and also such impurities may lead to concomitant shift of the lattice parameter. Electrochemical growth of ZnO from $Zn(ClO_4)_2$ and $Zn(NO_3)_2$ follows different mechanisms. When ZnO is deposited from $Zn(ClO_4)_2$, the reduction of dissolved O_2 leads to the formation of higher concentration of hydroxide first and then ZnO. But for ZnO deposited from $Zn(NO_3)_2$, the reduction of the nitrate ion was catalyzed by the presence of Zn^{2+} ions.²⁴ Hence, ZnO nanowire arrays grown from

$Zn(NO_3)_2$ solution might have higher oxygen defects. This oxygen defects variation in the nanowire arrays may be responsible for the blueshift. For instance, ZnO nanowire arrays grown from $Zn(NO_3)_2$ solution in the presence of hydrogen peroxide show redshift in the optical band gap [Fig. 3(b)]. Although doping ZnO with metal ions shows bigger variation in the optical band gap, electrochemical deposition offers a simple approach to fabricate nanowire arrays with the possibility of tuning the band gap.

In summary, homoepitaxial growth of vertically aligned ZnO nanowires on the seeded ITO substrate at low temperature (70 °C) from an electrolyte aqueous bath using electrochemical reactions has been described. The preparation method is template-free and can be grown on any conducting substrate. Optical measurement shows high transmittance in the visible range due to good crystallinity of the nanowire. Significantly, the aligned ZnO nanowire arrays fabricated from $Zn(ClO_4)_2$ and $Zn(NO_3)_2$ solution exhibit different optical band gaps and offer easy way to fine tune the optical band gap of the aligned ZnO nanowire arrays.

This work was supported by the National Creative Research Initiative Program supported by Korea Organization of Science and Engineering Foundation and The Second Stage of Brain Korea 21 Project.

¹D. Appell, *Nature (London)* **419**, 553 (2002).

²L. Samuelson, *Mater. Today* **6**, 22 (2003).

³X. F. Duan, Y. Huang, Y. Cui, J. F. Wang, and C. M. Lieber, *Nature (London)* **409**, 66 (2001).

⁴D. EzgFr, Ya. I. Alivov, C. Liu, A. Teke, M. A. Reshchikov, S. Doğan, V. Avrutin, S.-J. Cho, and H. MorkoA, *J. Appl. Phys.* **98**, 041301 (2005).

⁵A. Tsukazaki, T. Onuma, M. Ohtani, T. Makino, M. Sumiya, K. Ohtani, S. F. Chichibu, S. Fuke, Y. Segawa, H. Ohno, H. Koinuma, and M. Kawasaki, *Nat. Mater.* **4**, 42 (2005).

⁶M. Law, L. E. Greene, J. C. Johnson, R. Saykally, and P. Yang, *Nat. Mater.* **4**, 455 (2005).

⁷J. J. Wu, and S. C. Liu, *Adv. Mater. (Weinheim, Ger.)* **14**, 215 (2002).

⁸H. Yuan and Y. Zhang, *J. Cryst. Growth* **263**, 119 (2004).

⁹W. I. Park, D. H. Kim, S.-W. Jung, and G.-C. Yi, *Appl. Phys. Lett.* **80**, 4232 (2002).

¹⁰L. Vayssieres, *Adv. Mater. (Weinheim, Ger.)* **15**, 464 (2003).

¹¹L. E. Greene, M. Law, D. H. Tan, M. Montano, J. Goldberger, G. Somorjai, and P. Yang, *Nano Lett.* **5**, 1231 (2005).

¹²R. Liu, A. A. Vertegel, E. W. Bohannon, T. A. Sorenson, and J. A. Switzer, *Chem. Mater.* **13**, 508 (2001).

¹³T. Pauporté, D. Lincot, B. Viana, and F. Pellé, *Appl. Phys. Lett.* **89**, 233112 (2006).

¹⁴Y. Li, G. W. Meng, L. D. Zhang, and F. Philipp, *Appl. Phys. Lett.* **76**, 2011 (2000).

¹⁵T. Pauporté and D. Lincot, *Electrochim. Acta* **45**, 3345 (2000).

¹⁶R. Jayakrishnan and G. Hodes, *Thin Solid Films* **440**, 19 (2003).

¹⁷Z. Liu, Z. Jin, J. Qiu, X. Liu, W. Wu, and W. Li, *Semicond. Sci. Technol.* **21**, 60 (2006).

¹⁸Q.-Ping Chen, M.-Z. Xue, Q.-R. Sheng, Y.-G. Liu, and Z.-F. Ma, *Electrochem. Solid-State Lett.* **9**, C58 (2006).

¹⁹T. Yamamoto, T. Shiosaki, and A. Kawabata, *J. Appl. Phys.* **51**, 3113 (1980).

²⁰S. Peulon and D. Lincot, *J. Electrochem. Soc.* **145**, 864 (1998).

²¹E. A. Dalchiele, P. Giorgi, R. E. Marotti, F. Martín, J. R. Ramos-Barrado, R. Ayouchi, and D. Leinen, *Sol. Energy Mater. Sol. Cells* **70**, 245 (2001).

²²Y. S. Wang, P. J. Thomas, and P. O'Brien, *J. Phys. Chem. B* **110**, 21412 (2006).

²³Y. S. Wang, P. J. Thomas, and P. O'Brien, *J. Phys. Chem. B* **110**, 4099 (2006).

²⁴T. Yoshida, D. Komatsu, N. Shimokawa, and H. Minoura, *Thin Solid Films* **451-452**, 166 (2004).